

The new approach led to a reduction in the complexity of the gain prediction module of ~92%. This means a 20% reduction in the overall computational load of the codec, which is ~25 MIPS.

Subjective listening tests: To evaluate the efficiency of this new method, we carried out a series of listening tests using several speech sequences of different speakers, both male and female, in different environmental conditions.

Table 2 gives the percentage of preferences expressed by 30 listeners between the standard version of the codec and the modified version. It shows that most of the listeners did not perceive any difference between the two versions.

Conclusion: We have proposed a valid alternative for reducing the complexity of an LD-CELP speech codec. The novelty lies in the use of a fuzzy system for backward excitation gain prediction. We have shown that the new approach reduces the computational load of the module by ~92%, preserving the same perceptible speech quality as the traditional solution in various functioning conditions.

© IEE 1997

28 April 1997

Electronics Letters Online No: 19971289

F. Beritelli, S. Casale and A. Cavallaro (Istituto di Informatica e Telecomunicazioni - University of Catania, V. le A. Doria 6, 95125 Catania, Italy)

Corresponding author: S. Casale

E-mail: casale@iit.unict.it

References

- SCHROEDER, M., and ATAL, B.: 'Code excited linear prediction: high quality speech at low bit rates'. Proc. ICASSP, 1985, pp. 937-940
- ITU-T (CCITT) G.728: 'Coding of speech at 16 kbit/s using low-delay code excited linear prediction'. Recommendation G.728, September 1992
- CHEN, J., COX, V., CHUN LIN, Y., and JAYANT, N.: 'A low delay CELP coder for the CCITT 16kbit/s speech coding standard', *IEEE J. Sel. Areas Commun.*, 1992, 10, (5), pp. 830-849
- DAVIDSON, G., and GERSHO, A.: 'Complexity reduction methods for vector excitation coding'. Proc. IEEE Int. Conf. Acoustics, Speech and Signal Process., 1986, pp. 3055-3058
- TRANCOSO, I., and ATAL, B.: 'Efficient search procedures for selecting the optimum innovation in stochastic coders', *IEEE Trans. Acoustics Speech Signal Process.*, 1990, 38, (3), pp. 385-396
- ZADEH, L.A.: 'Fuzzy logic, neural networks and soft computing', *Comm. of ACM*, 1994, 37, (3), pp. 77-84
- RUSSO, M.: 'A genetic approach to fuzzy learning'. 1st Int. Workshop Neuro-Fuzzy Systems, EPFL, Lausanne, August 1996, pp. 9-16
- BERITELLI, F., CASALE, S., and RUSSO, M.: 'Robust phase reversal tone detection using soft computing'. Proc. ISUMA-NAFIPS, Maryland, USA, September 1995, pp. 589-594
- BERITELLI, F., CASALE, S., and RUSSO, M.: 'Multilevel speech classification based on fuzzy logic'. IEEE Workshop Speech Coding, Annapolis, USA, September 1995, pp. 97-98

Multidimensional cubic constellation with non-flat power spectrum

A.K. Khandani

Indexing terms: Multidimensional systems, Digital signal processing

The author presents a multidimensional cubic constellation with a non-flat power spectrum. The objective is to maximise the rate for a fixed average energy, subject to certain constraints on the resulting power spectrum.

Introduction: Consider the block diagram shown in Fig. 1. The N - D base-band constellation \mathbf{a} is bounded within a cubic region \mathbf{C}_a . Using a continuous approximation, the normalised rate of \mathbf{a} is computed as

$$H(\mathbf{a}) = \log[V(\mathbf{C}_a)] \quad (1)$$

where $V(\mathbf{C}_a)$ is the volume of \mathbf{C}_a .

The average energy along the i th dimension of \mathbf{C}_a is denoted as λ_i , where $\lambda_i > 0$. We define $\Lambda_a = \text{diag}[\lambda_0, \dots, \lambda_{N-1}]$. Each signalling interval (block) is composed of N_m time periods $N_m \geq N$. The total average energy per block is normalised to N_m , resulting in $\sum \lambda_i = N_m$.

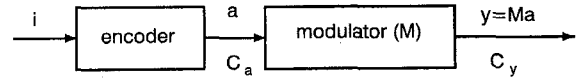


Fig. 1 System block diagram

The columns of the $N_m \times N$ matrix \mathbf{M} are the dimensions of the constellation \mathbf{y} ($\mathbf{M}\mathbf{M} = \mathbf{I}$ where \mathbf{I} is the $N \times N$ identity matrix). For $N < N_m$, we can have up to $N_m - N$ nulls in the power spectrum of \mathbf{y} .

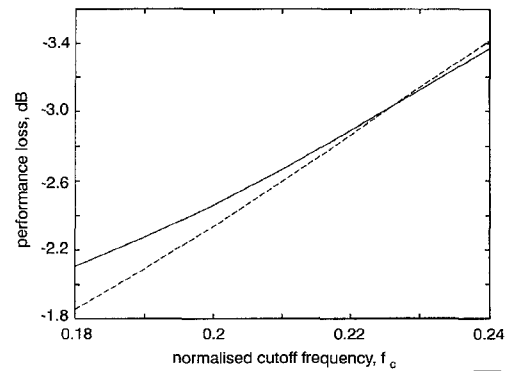


Fig. 2 Performance loss against $f_c = \omega_c/2\pi$, with and without spectral null, for the case of optimised basis

$F_p = 0.1$, $N_m = 4$

--- no spectral null, optimised basis

— spectral null, optimised basis

Defining $\mathbf{R}_y = \mathbf{E}[\mathbf{y}\mathbf{y}^T]$, it can be shown that

$$H(\mathbf{y}) = \frac{N}{2} \log(12) + \frac{1}{2} \sum_{\lambda_i(\mathbf{R}_y) \neq 0} \log[\lambda_i(\mathbf{R}_y)] \quad (2)$$

where $\lambda_i(\mathbf{R}_y)$ is the i th eigenvalue of \mathbf{R}_y . Assuming that all the eigenvalues are nonzero, we obtain $\sum_i \log[\lambda_i(\mathbf{R}_y)] = \log(|\mathbf{R}_y|)$ where $|\cdot|$ denotes the determinant. To realise a given \mathbf{R}_y , we select \mathbf{M} and Λ_a as the matrices of the eigenvectors and eigenvalues of \mathbf{R}_y , respectively.

Using the results of [1], the power spectrum of \mathbf{y} is equal to

$$\begin{aligned} S_y(\omega) &= \frac{1}{N_m} \sum_{k=0}^{N_m-1} \sum_{|i-j|=k} R_y(i, j) \cos(\omega k) \\ &= \frac{1}{N_m} \sum_{i=0}^{N-1} \lambda_i S_i(\omega) \end{aligned} \quad (3)$$

where $S_i(\omega)$ is the spectrum of the i th dimension. Given a cutoff frequency ω_c , we define the power-ratio of a spectrum as the fraction of the energy in the frequency band $[0, \omega_c]$. The F_p -constraint is to have a power-ratio $\leq F_p$. Integrating eqn. 3, the F_p -constraint is expressed as

$$\sum_{k=0}^{N_m-1} \sum_{|i-j|=k} R_y(i, j) \sin(\omega_c k)/k \leq \pi N_m F_p \quad (4)$$

In the case of spectral null(s), we consider \mathbf{y} as the output of a linear system \mathbf{A} with the same null(s) and reformulate the problem at the system input \mathbf{x} . As \mathbf{x} has no spectral null, \mathbf{R}_x is positive-definite. Using $\mathbf{R}_y = \mathbf{A}\mathbf{R}_x\mathbf{A}^T$, to maximise $H(\mathbf{y})$, we should maximise $|\mathbf{R}_x|$. In this case, the energy constraint and the F_p constraints transfer to:

$$\sum_{p=0}^{N-1} \sum_{q=0}^{N-1} U(p, q) R_x(p, q) = N_m$$

$$U(p, q) = \sum_{i=0}^{N_m-1} A(i, p)A(i, q) \quad (5)$$

$$\sum_{p=0}^{N-1} \sum_{q=0}^{N-1} W(p, q)R_x(p, q) \leq \pi N_m F_p$$

$$W(p, q) = \sum_{i=0}^{N_m-1} \sum_{j=0}^{N_m-1} A(i, p)A(j, q) \frac{\sin[\omega_c(i-j)]}{(i-j)}$$

The objective is to select \mathbf{M} and Λ_a to maximise the second term in eqn. 2 for $\sum \lambda_i = N_m$ subject to some constraints on the power spectrum of \mathbf{y} . It is easy to see that such spectral constraints translate into linear constraints on the elements of \mathbf{R}_x .

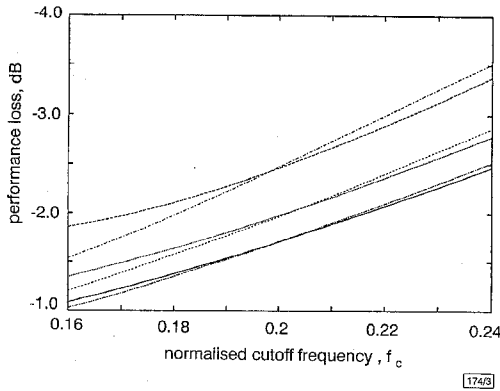


Fig. 3 Performance loss against $f_c = \omega_c/2\pi$, with and without spectral null, for the case of fixed basis

$F_p = 0.1$, $N_m = 4, 8, 16$
 - - - - $N_m = 4$, no null; — — — $N_m = 4$, null
 - - - - $N_m = 8$, no null; - - - - $N_m = 8$, null
 - - - - $N_m = 16$, no null; — — — $N_m = 16$, null

Optimum spectral shaping: Using the previous results, the final optimisation problem is as follows:

$$\begin{cases} \text{Maximise} & \log(|\mathbf{R}_x|) \\ \text{Subject to:} & \sum_{i=0}^{N-1} \sum_{j=0}^{N-1} B_l(i, j)R_x(i, j) \leq e_l \quad l \in [0, L-1] \\ & \mathbf{R}_x \text{ is symmetric positive-definite} \end{cases} \quad (6)$$

where L denotes the total number of spectral constraints. Using the results of ([2] p.467), it is easy to show that eqn. 6 is a convex optimisation problem. As a result, the maximum point is unique and can be computed using the Lagrange method.

We define an active constraint as a constraint for which the equality holds. The set of the active constraints are denoted by A_c . The Lagrange multipliers are denoted by ξ_l , $l \in A_c$. Calculating the derivatives with respect to the elements of \mathbf{R} , we obtain

$$\text{adj}[\mathbf{R}_x] = \sum_{l \in A_c} \xi_l \mathbf{B}_l \quad (7)$$

where $\text{adj}[\mathbf{R}_x]$ is the adjoint matrix of \mathbf{R}_x and \mathbf{B}_l is the matrix of the elements $B_l(i, j)$ in eqn. 6. For the spectral null constraint and the F_p constraint, we have $\mathbf{B} = \mathbf{U}$ and $\mathbf{B} = \mathbf{W}$, respectively, as given in eqn. 5. We also have

$$\mathbf{R}_x = |\text{adj}[\mathbf{R}_x]|^{\frac{1}{N-1}} \times (\text{adj}[\mathbf{R}_x])^{-1} \quad (8)$$

To calculate the Lagrange multipliers, we start from an initial value for the unknowns and compute \mathbf{R}_x using eqns. 7 and 8. Then, the status of the constraints is checked and the Lagrange multipliers are adjusted accordingly. This procedure is repeated in an iterative manner until the optimum solution is found.

It is easy to show that for the spectral nulls and/or the F_p -constraint, the energy constraint is always active. For $F_p \in [F_{min}, F_{max}]$ (given F_{min} and F_{max}), the F_p -constraint is active. For $F_p < F_{min}$, the optimisation problem has no answer. For $F_p > F_{max}$, the F_p -constraint is not active and the power-ratio remains at F_{max} . The F_{max} can be calculated by relaxing the F_p -constraint and finding the power-ratio of the resulting spectrum.

Spectral shaping with a fixed set of basis: This involves selecting a fixed M and using only Λ_a to maximise the rate. For a spectrum with spectral nulls, \mathbf{M} is selected as the output eigenvectors of a linear system with the same set of nulls. For the case of no spectral null, the sine basis is used. For a null at zero/Nyquist frequency, \mathbf{A} is taken as $1-D/1+D$ system (refer to [3] for the definition). The eigenvectors of these systems, given in [3], are closely related to the sine basis. This reduces the computational complexity of the modulation by using a fast sine transform algorithm.

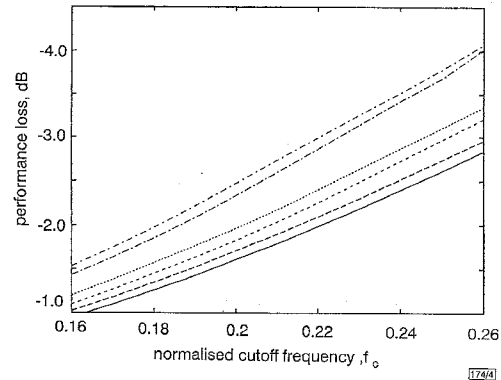


Fig. 4 Performance loss against $f_c = \omega_c/2\pi$, without spectral null, for cases of fixed and optimised basis

$F_p = 0.1$, $N_m = N = 4, 8, 16$
 - - - - fixed basis (sine), $N = 4$; — — — optimised basis, $N = 4$
 - - - - fixed basis (sine), $N = 8$; - - - - optimised basis, $N = 8$
 - - - - fixed basis (sine), $N = 16$; — — — optimised basis, $N = 16$

Using eqn. 3, the F_p -constraint is formulated as

$$\sum_{i=0}^{N-1} \lambda_i B_i(\omega_c) \leq \pi N_m F_p \quad B_i(\omega_c) = \int_0^{\omega_c} S_i(\omega) d\omega \quad (9)$$

As in the case of the optimised basis, the energy constraint is always active. This results in the following convex optimisation problem:

$$\begin{cases} \text{Maximise} & \sum_{i=0}^{N-1} \log(\lambda_i) \\ \text{Subject to:} & \sum_{i=0}^{N-1} \lambda_i B_i(\omega_c) \leq \pi N_m F_p \\ & \sum_{i=0}^{N-1} \lambda_i = N_m \quad \lambda_i \geq 0 \end{cases} \quad (10)$$

Assuming that the F_p -constraint is active and using the Lagrange method, we obtain

$$\lambda_i = \frac{1}{\xi_1 B_i(\omega_c) + \xi_2} \quad (11)$$

where ξ_1 and ξ_2 are determined by solving:

$$\sum_{i=0}^{N-1} \frac{B_i(\omega_c)}{\xi_1 B_i(\omega_c) + \xi_2} = \pi N_m F_p$$

and

$$\sum_{i=0}^{N-1} \frac{1}{\xi_1 B_i(\omega_c) + \xi_2} = N_m \quad (12)$$

In the case that the F_p -constraint is not active, the answer is obtained by allocating equal energy to all the dimensions.

Numerical results: In this Section, by a spectral null we mean a first-order null at zero frequency. For the sake of comparison, we consider a region C_0 which has N_m dimensions, with equal values of energy along each dimension. The increase in average energy of the region C_a with respect to the region C_0 , is measured by the factor P_l (performance loss). Figs. 2–4 show P_l against $f_c = \omega_c/2\pi$ for some cases of interest. It is seen that for high values of f_c , having a spectral null at zero frequency results in a better performance. The other conclusion is that increasing the space dimensionality can be very useful, specifically for higher values of f_c (having a wider null width).

References

- 1 CARIOLARO, G.L., and TRONCA, G.P.: 'Spectra of block coded digital signals', *IEEE Trans. Commun.*, 1974, **COM-22**, pp. 1555-1563
- 2 HORN, R.A., and JOHNSON, C.R.: 'Matrix analysis' (Cambridge University Press, 1985)
- 3 KHANDANI, A.K., and KABAL, P.: 'Block-based eigensystem of the 1±D and 1-D² partial-response channels', *IEEE Trans. Inform. Theory*, 1994, **40**, pp. 1645-1647

Prediction of propagation parameters in frequency hopping spread spectrum

M.P. Fitton, A.R. Nix and M.A. Beach

Indexing terms: Frequency hop communication, Spread spectrum communication

Frequency hopping spread spectrum (FH-SS) has found a number of applications in both CDMA and TDMA cellular systems, wireless local loop, and wireless local area networks. Propagation studies and statistical analysis are employed to show that the frequency hopped channel displays improved short-term characteristics when compared to the non-hopped case. Furthermore, novel analyses of the short-term statistics of the frequency-hopped channel enable prediction of the performance of an FH system.

Introduction: Frequency hopping spread spectrum (FH-SS) has been receiving a great deal of attention for a variety of applications in the field of wireless communications. The GSM worldwide digital standard incorporates frequency hopping to improve performance and ease frequency planning requirements [1]. Furthermore, the nature of the frequency-hopped channel is applicable in other areas, such as special mobile radio, wireless local loop, and wireless local area network technology. In particular, slow frequency hopping code division multiple access (FH-CDMA) has been found suitable as an air interface technique for flexible third generation wireless networks [2].

Frequency hopping improves short-term channel statistics, such as mean fade duration and level crossing rate. Consequently, it is unlikely that outage duration will be excessive. This effect can be exploited by interleaving the data, thus randomising error bursts and improving the performance of forward error correction (FEC). Alternatively, retransmission in an automatic repeat request (ARQ) scheme can occur on an uncorrelated hop frequency, thus maximising the throughput [3].

Theoretical and practical investigations of the frequency hopped mobile channel are employed in this Letter to characterise the impact of hopping on channel statistics. Previous propagation work [4] has indicated that frequency hopping does not alter the long-term statistics of the channel. Novel mathematical expressions governing the short-term statistics of the frequency-hopped channel are derived, enabling prediction of the overall performance of an FH system.

Measurement techniques: A campaign of frequency hopping propagation measurements was undertaken in an urban environment in the city of Bristol, at 1.823GHz [4]. A near-Rayleigh channel with a Doppler frequency of ~20Hz was studied over a 100m section. The coherence bandwidth of the channel corresponds to 1040kHz for a threshold of 0.5, and 250kHz for a threshold of 0.9 [4].

Level crossing rate: The level crossing rate (N_R) [5] is defined as the number of positive going transitions of the signal magnitude

with respect to a certain threshold, R . A high level crossing rate implies a rapidly changing channel, with problems arising from static nulls becoming statistically unlikely.

To simplify the analysis of level crossing rate in a frequency-hopped channel, it is assumed that the channel is constant over a hop period, so that the instantaneous characteristics due to channel variations can be neglected. For this assumption to be valid, it is necessary for the coherence time of the narrowband channel [6] to exceed the hop frame duration. The level crossing rate can then be calculated from the cumulative channel statistics both before and after a hop boundary (a Rayleigh distribution is assumed in this case [5]). To simplify analysis all frequencies are assumed to be uncorrelated, which results if the hop bin spacing exceeds the channel coherence bandwidth. The level crossing rate of a hopped channel is given by eqn. 1, where f_{hop} is the hop rate (in hops per second), R is the magnitude threshold level, and σ is the standard deviation of the random variable:

$$N_R = f_{hop}P[r_1 < R]P[r_2 > R] = f_{hop}e^{-R^2/2\sigma^2}(1 - e^{-R^2/2\sigma^2}) \tag{1}$$

Level crossing rate propagation results: Comparison of real and predicted statistics for non-hopped and hopped systems is shown in Fig. 1. The hopped system is operating at a rate of 500 hops per second, and adjacent frequencies are separated by 1.5MHz. The diagram indicates reasonable agreement between real and predicted data. In particular, the hopped performance is accurately predicted by eqn. 1 at high magnitude thresholds. At lower values, the statistics of the channel dominate, and thus the measured hopping characteristic tends towards the non-hopped theoretical curve. In particular, it is not necessarily valid to assume that the channel is stationary over the hop frame, as in eqn. 1.

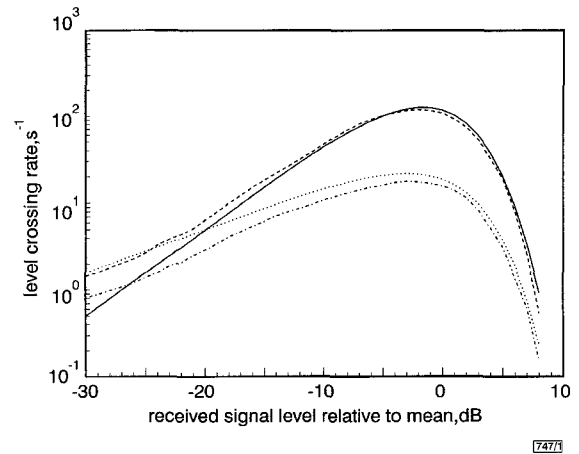


Fig. 1 Predicted and measured level crossing rate
 — predicted 500 hps; - - - measured 500 hps
 predicted non-hopped; - · - · measured non-hopped

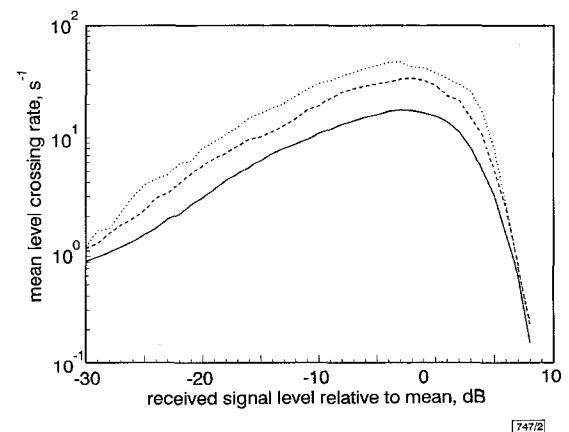


Fig. 2 Level crossing rate
 100 kHz spacing
 — CW; - - - 500 hps; 1000 hps